NUWC-NPT Technical Memorandum 972159
Copy 1

Naval Undersea Warfare Center Division
Newport, Rhode Island

ELF PLASMA ANTENNA

Theodore R. Anderson
Submarine Electromagnetic Systems Department

30 September 1997

Report Documentation Page

Form Approved
OMB No. 0704-0188

1. REPORT DATE	2. REPORT TYPE	3. DATES COVERED
30 SEP 1997	**Technical Memo**	**30-09-1997 to 30-09-1997**

4. TITLE AND SUBTITLE
ELF Plasma Antenna

5a. CONTRACT NUMBER

5b. GRANT NUMBER

5c. PROGRAM ELEMENT NUMBER

6. AUTHOR(S)
Theodore Anderson

5d. PROJECT NUMBER
93098

5e. TASK NUMBER

5f. WORK UNIT NUMBER

7. PERFORMING ORGANIZATION NAME(S) AND ADDRESS(ES)
Naval Undersea Warfare Center Division,1176 Howell Street,Newport,RI,02841

8. PERFORMING ORGANIZATION REPORT NUMBER
TM 972159

9. SPONSORING/MONITORING AGENCY NAME(S) AND ADDRESS(ES)

10. SPONSOR/MONITOR’S ACRONYM(S)

11. SPONSOR/MONITOR’S REPORT NUMBER(S)

12. DISTRIBUTION/AVAILABILITY STATEMENT
Approved for public release; distribution unlimited

13. SUPPLEMENTARY NOTES
NUWC2015

14. ABSTRACT
This effort is intended to stimulate further research and development of an extremely low frequency (ELF) plasma antenna. The study explores the advantages of a transmitting ELF plasma antenna for submarine applications and draws comparisons between this antenna and those currently in use. Three promising designs are discussed, and mathematical models used in this study are presented.

15. SUBJECT TERMS
Periscope Plasma Antenna; ELF; Extremely low frequency

16. SECURITY CLASSIFICATION OF:			17. LIMITATION OF ABSTRACT	18. NUMBER OF PAGES	19a. NAME OF RESPONSIBLE PERSON
a. REPORT	b. ABSTRACT	c. THIS PAGE			
unclassified	**unclassified**	**unclassified**	**Same as Report (SAR)**	**41**	

ABSTRACT

This effort is intended to stimulate further research and development of an extremely low frequency (ELF) plasma antenna. The study explores the advantages of a transmitting ELF plasma antenna for submarine applications and draws comparisons between this antenna and those currently in use. Three promising designs are discussed, and mathematical models used in this study are presented.

ADMINISTRATIVE INFORMATION

This memorandum was prepared under NUWC Division Newport Project No. 93098, "Periscope Plasma Antenna," principal investigator Theodore R. Anderson (Code 3431).

ACKNOWLEDGMENT

The author is grateful for the support of Richard H. Nadolink (Code 10), the program management of Robert J. Aiksnoras (Code 3491), helpful discussions with John Casey (Code 3413), and the receptiveness of Peter M. Trask (Code 34) to the ELF plasma antenna concept.

TABLE OF CONTENTS

LIST OF ILLUSTRATIONS

LIST OF TABLES

ELF PLASMA ANTENNA

1. INTRODUCTION

The extremely low frequency (ELF) plasma antenna concept grew primarily from five areas: (1) the corona mode ELF antenna, the properties of which depend on ionization of the air around a vertical ELF antenna suspended by a balloon in air; (2) the Naval Research Laboratory (NRL) reflector plasma antenna, which is currently being tested; (3) a 1966 patent entitled "Laser Beam Antenna"; (4) a 1965 report (prepared by the American Nucleonics Corporation (ANC)) on the plasma antenna as a receiver in a nuclear environment; and (5) mathematical proof of farfield radiation by oscillating plasmas.

This effort draws on knowledge and experience gained in these five areas to conceive and design a transmitting ELF plasma antenna that, if implemented, would have a tremendous impact on submarine ELF communications: the convenience of antenna transportability would replace unwieldy vertical electric dipole ELF antennas, balloons suspended in air, and inefficient horizontal electric dipole ELF antennas.

In this study various designs were explored to develop an ELF plasma antenna, and at least three designs show promise. One system, which would use the reflective properties of plasmas to redirect a radar signal, is under development by NRL. NRL has devised a plasma sheet (which currently is mechanically rotated) to reflect a high-frequency signal radiated by a driving antenna (see figure 1). The device is designed primarily for surface ship applications. A future system could steer the plasma sheet electronically, which would result in a fast, multifunctional antenna reflector.

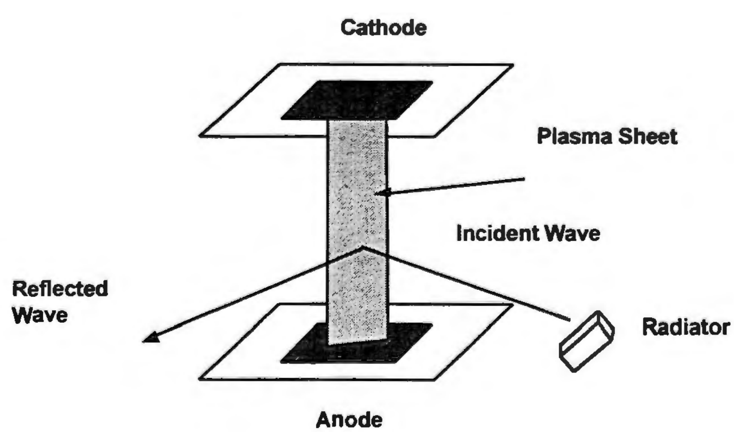

Figure 1. NRL Plasma Reflector

Another potential application of the reflective/transmission properties of the plasma is the reduction of the radar cross section of an antenna. These properties can reduce the size of the radar cross section as long as the plasma antenna is operating at a frequency below that of search radars. The reduction might be minimal because the mounting structure usually reflects more radar signals than the actual antenna element, but even some reduction is important for submarine application if the antenna is mounted on top of the mast or combined as a conformal antenna on a stealth sail.

The reduced cross section is probably of greater importance to the surface ship community, where the antennas tend to be relatively large and can contribute significantly to the size of the ship cross section. For example, in a case where the plasma antenna is transmitting at a frequency of 30 MHz and is scanned by a radar operating at 3 GHz, the amount of reflected energy would be on the order of 0.047 percent. With no physical structures supporting the ELF plasma antenna, its radar cross section will be zero because its natural resonance frequency will always be less than the radar frequency; the antenna can therefore be operated in regions where undetectability is desirable.

Currently, the operating ELF antenna is the horizontal electric dipole (HED) antenna. However, horizontal ELF antennas are extremely inefficient and must be located where large regions of low ground conductivity exist. The vertical electric dipole antenna, with and without corona, is much more efficient but is aerostat-supported, unwieldy, and subject to "blowdown," which causes this tethered antenna to assume the form of a catenary. The vertical electric dipole ELF antenna is experimental and has not been implemented.

2. ELF PLASMA ANTENNA CONCEPT

The ELF plasma antenna concept uses as a current carrier an ionized column of air, created by one or more lasers, with a length on the order of the vertical electric dipole (with or without corona) ELF antenna. The vertical length can be 12,500 ft, as it was for the vertical electric dipole ELF antenna; 5.2 km, as in the corona mode antenna; or ideally, as in some of the proposed designs, all the way to the ionosphere (30 km to 70 km). In several designs, this ionized column of air is forced to oscillate at ELFs.

One of the most promising designs uses a high-powered laser to ionize a pencil-thin column of air and to control the oscillation by momentum transfer of laser photons to charge carriers in the ionized column, which affect an upward current by momentum transfer and a downward current by laser controlled gravitational relaxation. An alternate method, using pure laser control of the level of ionization and current oscillation, is to use electro-optic modulation of the ionizing laser beam to send an ELF wave along the ionized column. The electro-optic modulation can be achieved by passing the laser beam through an electro-optic crystal, with an ELF oscillating voltage applied transversely to the crystal. By ionizing a thin column all the way to the ionosphere and sending an ELF oscillation along this column by electro-optic modulation, this oscillation can be reflected from the ionosphere and a resonance ELF antenna can be created.

The development of some designs has examined the possibility of an external electric field oscillating at ELFs and driving the plasma column. This could be achieved by using an oscillating electric field from an antenna at the base and focusing the electric field with an electrostatic lens. Other designs have included the use of acoustic waves to drive the charge carriers in the plasma.

2.1 PLASMA ANTENNA: A RECEIVING DEVICE

Research performed by the ANC in 1965 (sponsored by the Defense Atomic Support Agency) demonstrated the ability of a plasma column to act as a receiving antenna (ANC, 1965). The objective of the project was to develop an antenna to measure the radiated electric field produced by a nuclear explosion. Alternate antenna designs were sought because traditional metallic antennas were adversely affected by the ionizing radiation produced by the nuclear event. The antenna prototype developed by ANC is essentially a propane torch seeded with cesium or barium. The additives provide the flame with a variable conductive component. Because the flame is conductive, electromagnetic (EM) signals couple to the plasma and are received via a cathode follower pickup wire located within the flame. The wire attracts electrons that give rise to a received voltage. The received wire is connected to a traditional spectrum analyzer to measure the induced voltage.

Measurements performed on this design showed that the propane plasma behaved like a whip antenna. The frequency response was linear between 50 kHz and 50 MHz. The researchers suggested that the low-frequency response of the antenna could be improved by increasing the conductivity of the flame (e.g., increasing the cesium concentration).

The sensitivity of the propane plasma antenna was measured and compared to the performance of a 14-in. whip antenna. The results of these measurements are illustrated in figure 2, which shows the received signal (terminal voltage) of the plasma and whip antennas as a function of the generator voltage at the driving antenna; the plasma antenna appeared to be more efficient than the whip. This, however, could be attributed to the size of the flame, which might have been larger than the 14-in. whip antenna, resulting in a larger capture area (the size of the flame was not specified). A portion of the study was also devoted to developing an equivalent circuit model of the ANC plasma antenna; the final model, illustrated in figure 3, provides a relationship between the resistance and capacitance of the plasma and the received voltage.

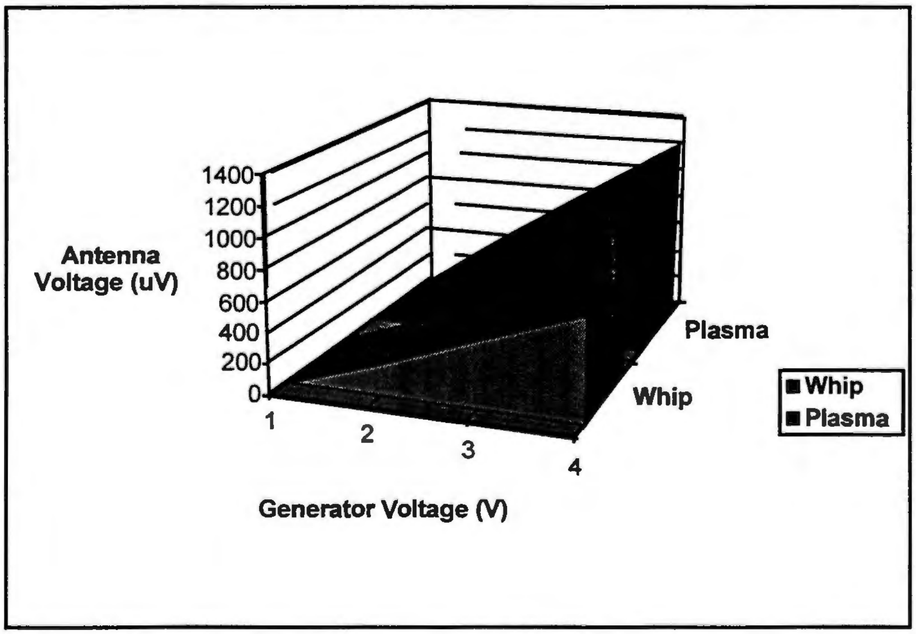

Figure 2. Comparison of Reception of ANC Plasma Antenna vs. 14-in. Whip Antenna

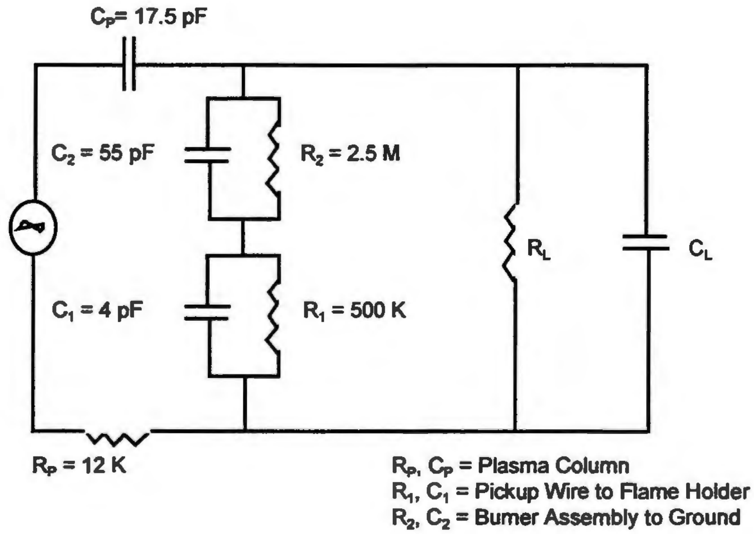

Figure 3. Equivalent Circuit Model of Plasma Antenna

2.2 IONIZATION LEVELS AND ENERGY REQUIREMENTS FOR CREATION OF AN IONIZED COLUMN IN THE ATMOSPHERE BY LASERS

The primary chemical composition of air is shown in table 1. Since the density of air decreases with increasing height, the corresponding energy required to ionize the column will also decrease at different heights. The atmospheric density at different altitudes is listed in table 2 (Roussel-Dupré and Miller, 1993b).

Table 1. Composition of Air

Element	Molecular Weight	Percent by Volume	Percent by Weight	First Ionization Potential (eV)
Nitrogen	$N_2 = 28.0$	78.09	75.55	14.53
Oxygen	$O_2 = 32.0$	20.95	23.13	8.5
Argon	Ar = 39.944	0.93	1.27	15.755
Carbon Dioxide	$CO_2 = 44.010$	0.03	0.05	

Table 2. Atmospheric Density vs. Altitude

Height (m)	Density (kg/m^3)
0	1.225
800	1.156
1600	1.069
2400	0.967
3000	0.891
4000	0.819

For this effort, only the ionizing of a volume of nitrogen is considered. The ionization potentials in eV and joules are illustrated in figures 4 and 5. The energies shown reflect the values required to reach the first ionization potential. The energy required to achieve correspondingly higher ionization states can be computed by substituting the appropriate ionization potentials to the above equations. The charts can be used in conjunction with the parameters of existing lasers in order to estimate the size of the ionized spheres (e.g., when the lasers are used to ionize a spot). The densities in table 2 were substituted into the previously described equations to estimate the energy required to ionize a 1-cm^3 volume of nitrogen at varying heights. The results are illustrated in figures 6 and 7 for both eV and joules.

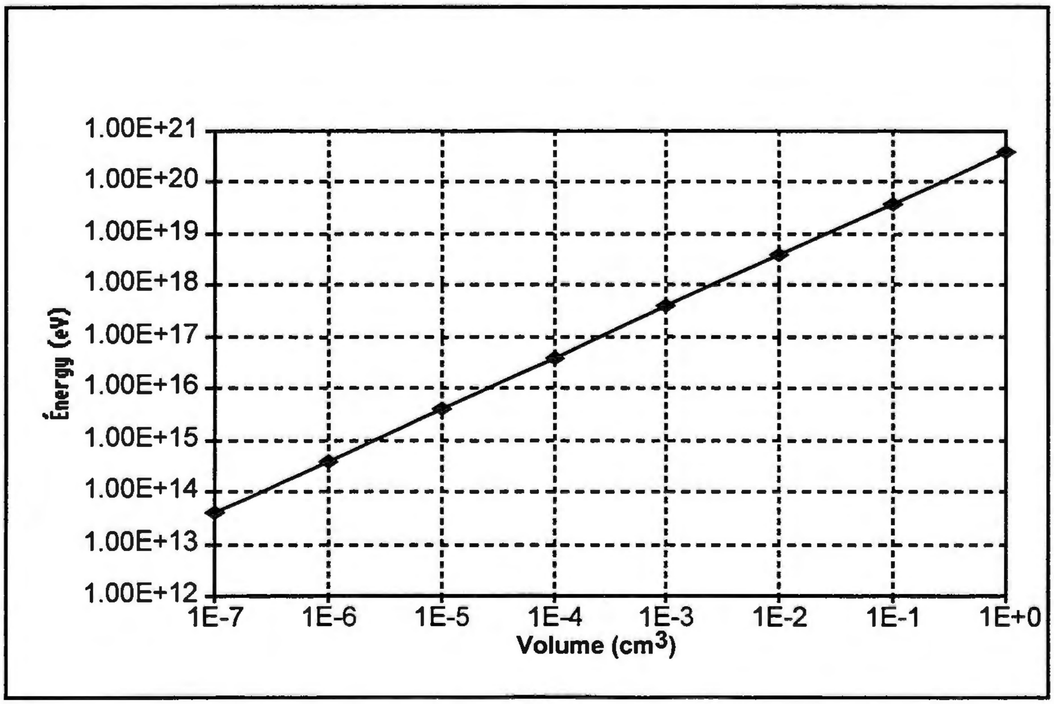

Figure 4. Ionization Potential (eV) vs. Volume for Nitrogen

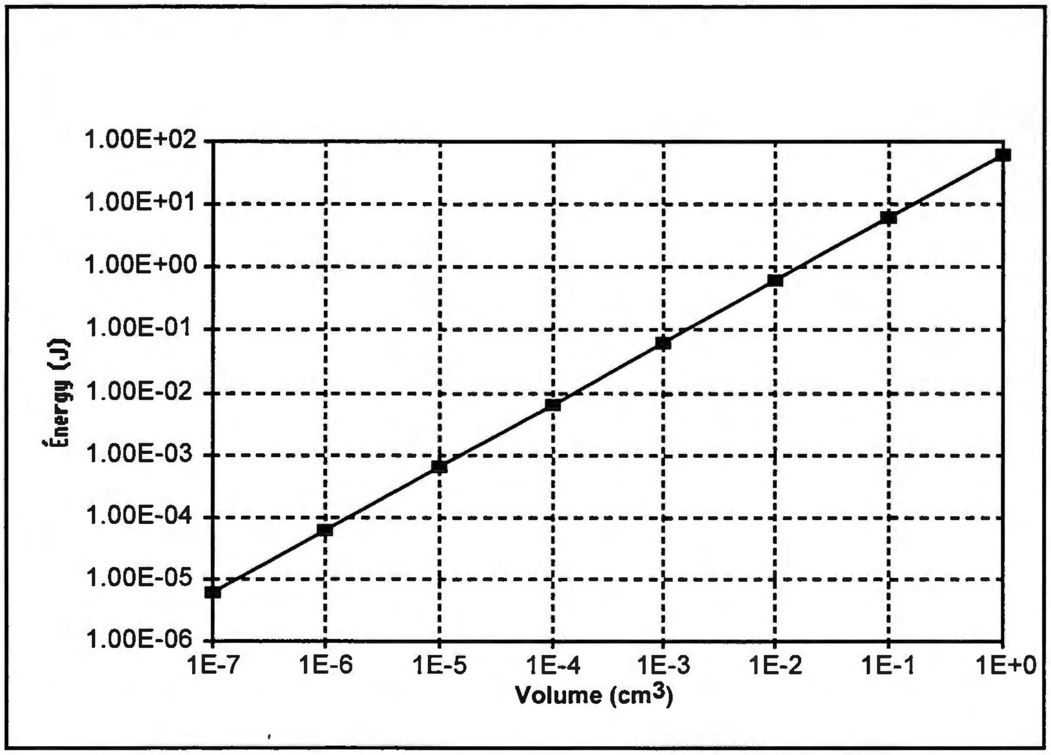

Figure 5. Ionization Potential (J) vs. Volume for Nitrogen

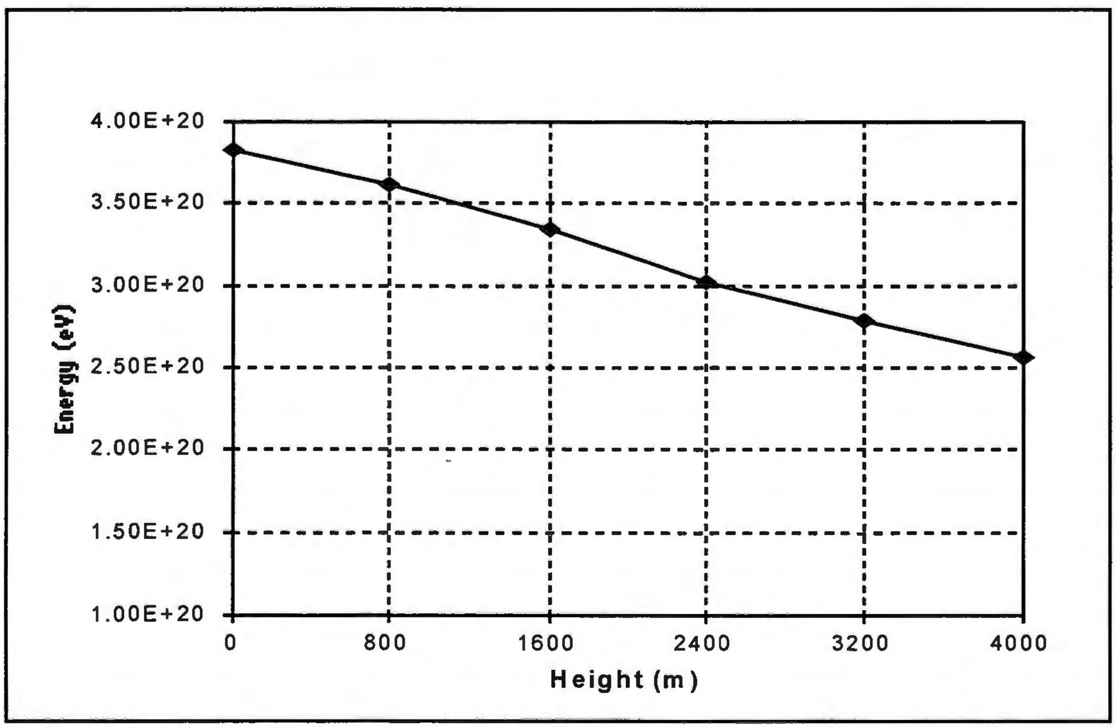

Figure 6. Ionization Energy (eV) for 1 cm^3 vs. Height Above Ground

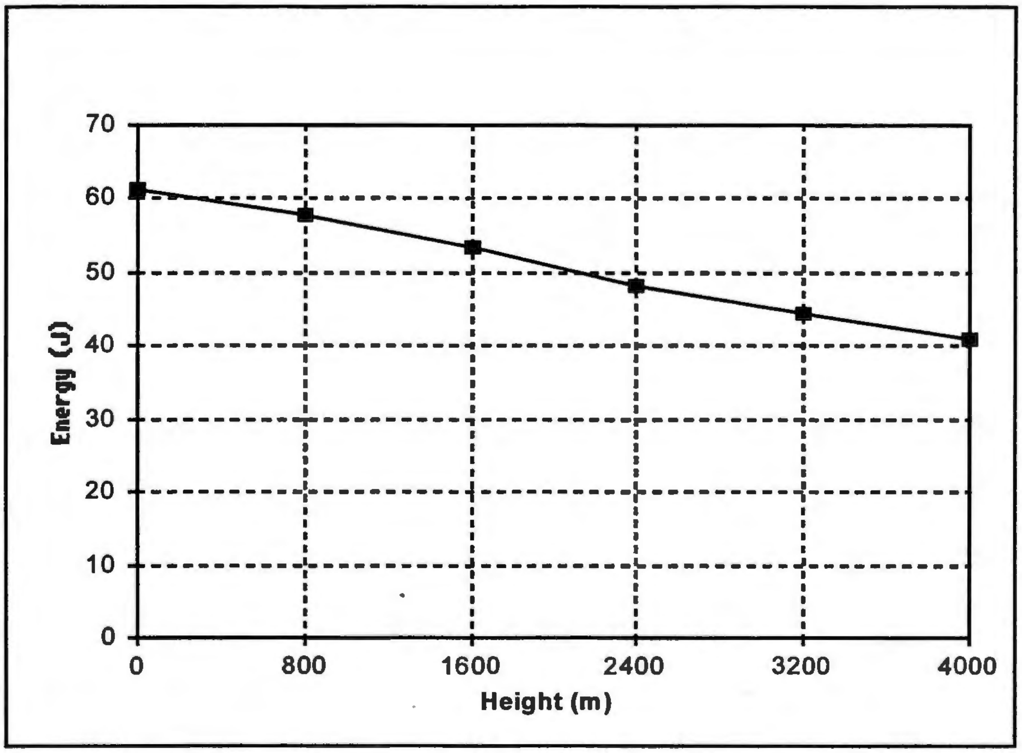

Figure 7. Ionization Energy (J) for 1 cm³ vs. Height Above Ground

2.3 AIR IONIZATION OF THE PLASMA COLUMN

The approach for computing the ionization potential is to determine the number of atoms in a given volume. The ionization potential for the volume is then computed as the product of the number of atoms times the ionization potential, which can be done using the equation for the speed of molecules (V) (Roussel-Dupré, 1993a), given as

$$V_{rms} = \sqrt{\frac{3p}{\rho}},$$

where p = pressure (1.01×10^5 N/m = 1 atm) and r = density (kg/m^3). This can be arranged to solve for the density r, which yields

$$\rho = \frac{3p}{V^2 \text{rms}}.$$

Velocities for nitrogen, oxygen, and air are (Halliday and Resnick, 1986):

Molecule	V_{rms} (m/s)
N_2	493
O_2	461
Air	485

The computed densities for nitrogen and oxygen are 1.2466 kg/m^3 and 1.426 kg/m^3, respectively. These results compare favorably with the tabular values provided in the *CRC Handbook of Engineering* (N = 0.0013 g/cm^3 and O = 0.0014 g/cm^3). The number of atoms per unit volume is computed as

$$N_{N_2} = \frac{\rho N_A}{A_N} ,$$

where N_A = Avogadro's number (6.023×10^{23}) and A_N = atomic weight.

Converting the values to the appropriate units yields the following:

$N_2 = 2.68 \times 10^{19}$ atm/cm^3
$O_2 = 2.684 \times 10^{19}$ atm/cm^3.

The energy required to ionize the volume is given as $e(ev) = V_{ion} N_{N2}$, where V_{ion} is ionization potential.

3. PRODUCTION OF ELF CURRENTS

The particle picture of laser photons shows that a photon has momentum and can exchange that momentum with solid matter. Hence, it is possible to drive ions or electrons in a given direction by colliding them with photons. This is the idea behind creating current in a plasma with the use of a laser as a driver. The photons can be made to be absorbed selectively by the ions and driven through inelastic collisions in the upward direction. The laser can do this over one-half the ELF period, after which the rapid relaxation of the ions and electrons to their respective Maxwell-Boltzman distributions takes place. The relaxation time period exceeds an ELF period, but the laser can be used to slow the relaxation time down to half an ELF period by transferring the right amount of momentum from the photons to the ions. Hence with the use of the laser exclusively, an ELF current can be created in the ionized column. (The relaxation time calculations and the momentum transfer equations are provided in the appendix.) Figure 8 shows the design and physical concepts.

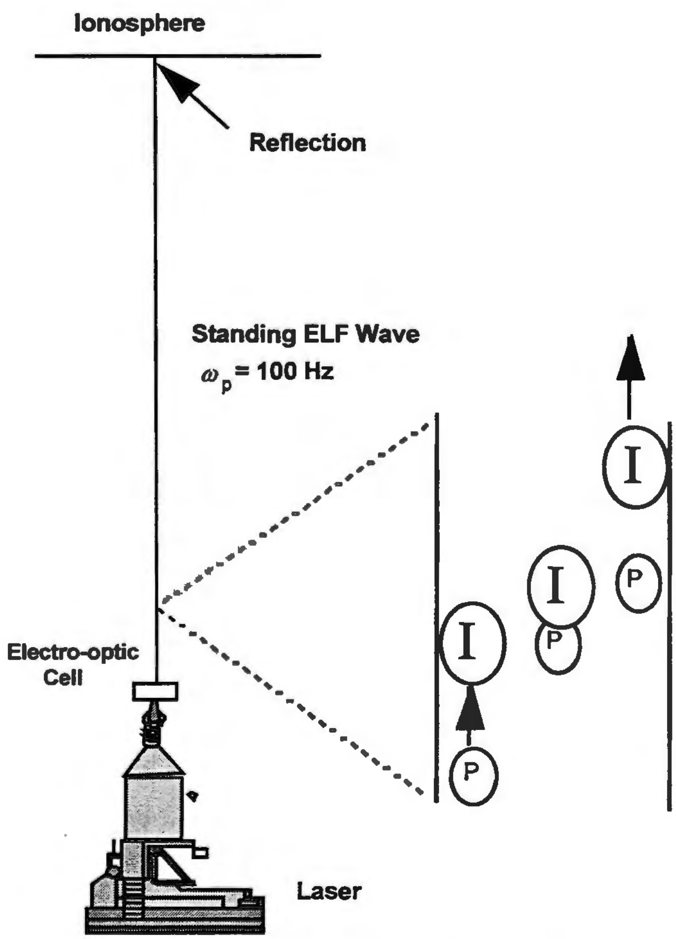

Figure 8. Laser-Induced ELF Plasma Antenna with Current Produced by Photon Momentum Exchange and Maxwellian Relaxation

3.1 LASER AS AN IONIZATION SOURCE

Modulation of laser beams by electro-optic crystals is a well-known technology that can be used to make the ionized column of air oscillate at ELFs. In this method a laser beam passes through an electro-optic crystal with electrodes attached to a voltage source that oscillates at the rotational frequency (RF). This causes the laser to carry an ELF wave that forces the charge carriers in the plasma to oscillate at the ELF and, hence, to radiate an ELF signal. To create a resonance ELF antenna, this wave must be reflected at the endpoint of the plasma antenna, which occurs because the natural resonance frequency of the ionosphere exceeds the ELF. This, in turn, causes the plasma ELF wave to reflect off the ionosphere and travel to Earth, producing a resonance antenna. Figures 9 and 10 illustrate this process.

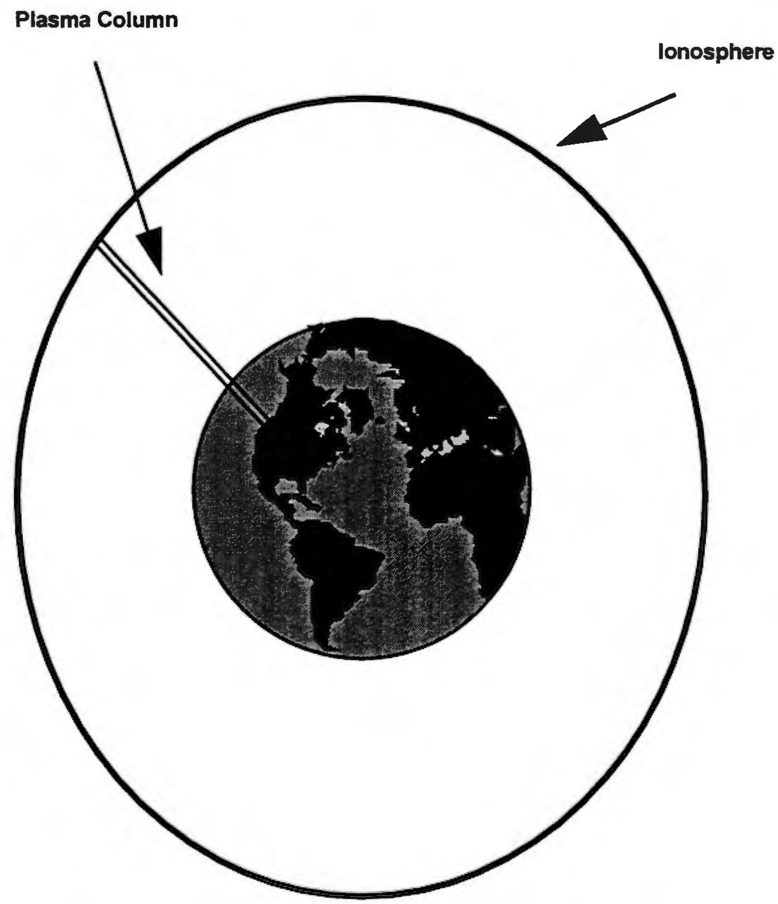

Figure 9. Use of the Ionosphere to Give Resonance Standing Wave Plasma Current

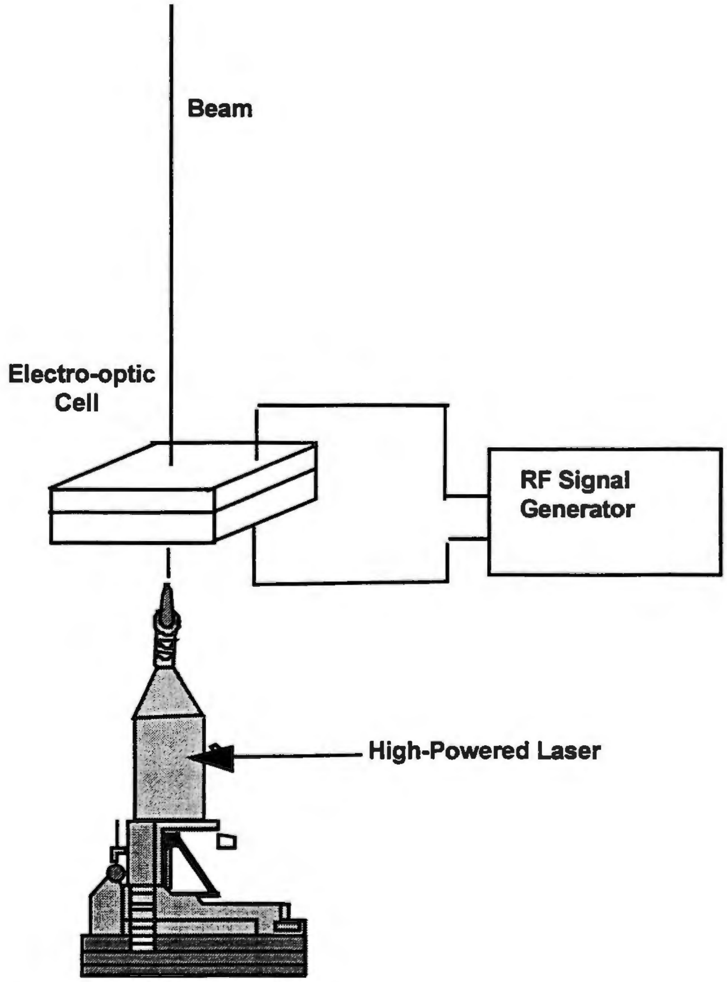

Figure 10. Laser-Produced Resonance Columns on the Plasma Column

3.2 EXTERNAL ACOUSTIC AND INTERNAL ION-ACOUSTIC DRIVEN PLASMA COLUMN ELF CURRENTS

Acoustic waves have the same physical properties (for the same frequencies) as EM waves, but they have much shorter wavelengths. Acoustic oscillations, therefore, are able to drive the charge carriers in a plasma at ELFs over a shorter distance than are EM oscillations. This eliminates the need for an aerostat-supported ELF transmitter, but the ion-acoustic antenna must be thicker in order to ensure a similar dipole moment as the aerostat-supported ELF antenna. The plots in figure 14 give the cross-sectional area of these types of antennas if the efficiency of the antennas is 100 percent—the conversion of input acoustic energy to output EM energy is done without losses to, say, Bremstralung. If the plasma is excited externally by an acoustic wave, the acoustic wave becomes an ion-acoustic wave in the plasma. The ion-acoustic wave is a longitudinal pressure wave in which the ions provide the inertia and the electrons provide the restoring force; hence, the ion-acoustic wave is an ion oscillation. At the ion resonance frequency, the ions have much more charge density than do electrons oscillating at the electron resonance frequency. Consequently, the ions oscillating at resonance and set to equal ELF can provide greater charge movement and a greater dipole moment than the electrons can.

The other attractive feature of the ion-acoustic design, shown in figure 11, is that the plasma can be contained in a structure. The ionization can be controlled by three methods: electrodes at each end, microwave heating, and laser ionizing. There is much more control over the ionization in this column than there is in other designs because it is much shorter and can be contained in a tube.

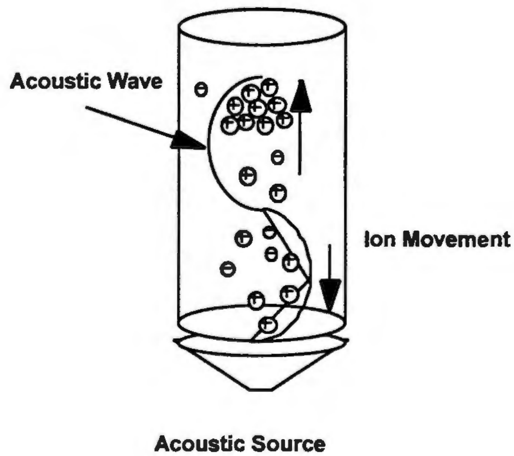

Figure 11. Ion-Acoustic Plasma Antenna

The acoustically driven plasma antenna design uses acoustic waves as the transport mechanism for the electrons and ions. The basic theory of the system is that the longitudinal acoustic waves propagating through a fluid (or plasma) medium result in pressure gradients that in turn result in particle movement. In this case, the particles are ions and electrons, and the movement will give rise to a radiated EM wave.

The plasma column will be significantly shorter than if the transport mechanism is attributed to an electric field, so it is conceivable that the ionization can be generated using either lasers or radio frequency (vibrational and rotational excitation). The conceptual view of the system is illustrated in figure 12.

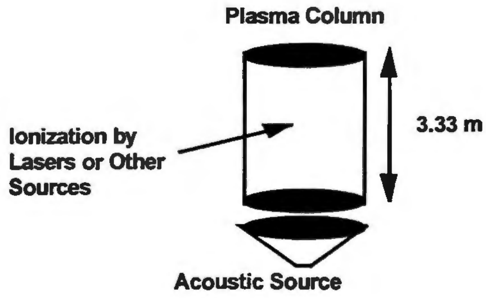

Figure 12. Acoustic Plasma Antenna

The acoustic source is essentially a low-frequency signal generator/amplifier combination that modulates a transducer. In this configuration, the acoustic source generates a wave that "pushes" and "pulls" the ions and electrons, thus creating movement. An example of the particle movement in a fluid medium is illustrated in figure 13, which shows that particles in a fluid (plasma in this case) cycle through compression, displacement, and re-refraction as the acoustic wave propagates through the medium. As the amplitude of the acoustic wave increases (e.g., at point p'), the plasma will start to compress to the right of point p'.

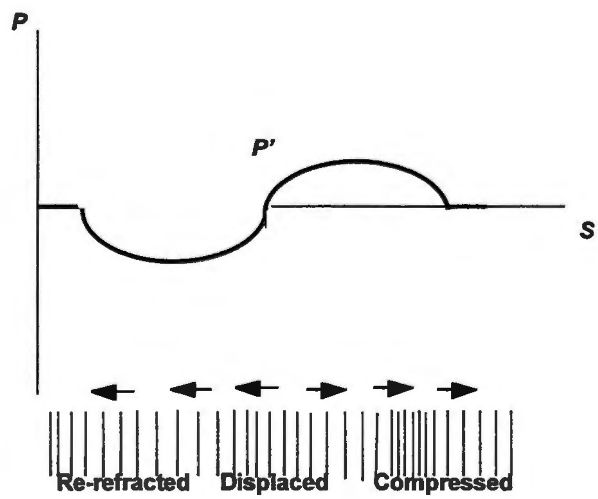

Figure 13. Acoustic Wave Interaction with Plasma

The compressed plasma increases the pressure on the region of the compressed particles, which in turn results in a pressure gradient in the -*s* direction, causing the particles to accelerate in the +*s* direction. The acceleration increases until the peak pressure point arrives, after which the compression (hence, pressure) subsides and velocity of the plasma begins to decrease. The velocity slows to zero as the acoustic wave begins the second half of its cycle. As the negative portion of the waveform increases, the backward velocity of the particles begins to increase, and it continues to increase until the negative peak is reached. The velocity then slowly returns to zero as the ambient line is crossed (Roussel-Dupré and Miller, 1993a).

The effect of the acoustic wave on the ions in the plasma column is shown in figure 11, which illustrates the particle compression and subsequent movement of the ions as the acoustic wave propagates up the column. The acoustic wave produces both forward and backward movement.

Sample calculations to determine the height of the plasma tube have been performed. The relationship between velocity, wavelength, and frequency of an acoustic wave is given as

$$\lambda_a f_a = V_a,$$

where V_a = acoustic velocity (333 m/s), λ_a = acoustic wavelength, and f_a = acoustic frequency (100 Hz). Assuming an ELF of 100 Hz, the wavelength of the acoustic wave is given as

$$\lambda a = \frac{333\,\mathrm{m/s}}{100\,\mathrm{Hz}} = 3.33\,\mathrm{m}.$$

This implies that as long as the plasma column is at least 3.33 m long, it should be capable of radiating an EM signal at the acoustic frequency. The result is a wavelength that can be realized with a relatively short plasma column.

Setting a standing acoustic wave on the plasma column causes the ions to move at approximately the acoustic frequency and the electrons to move at another frequency (to be determined). The electrons can move at a different velocity because of their smaller masses.

The next issue of concern is the signal generated by the plasma column. Assuming a sinusoidal wave, the acoustic pressure is expressed as (Roussel-Dupré and Miller, 1993a)

$$P = P_{pk}\cos(\omega t - kz + \phi),$$

the acoustic particle velocity (ions) as

$$r_v = \frac{z}{\rho c} P_{pk}\cos(\omega t - kz + \phi),$$

and the acoustic intensity as

$$I = \frac{P^2}{\rho c}.$$

The ions oscillate and cause radiation at the acoustic frequency.

The acoustic power is given as

$$P_{ac} = \text{Acoustic Power} = \frac{P^2}{\rho c} A,$$

where A is the cross-sectional area of the plasma column.

As a result of conversion of energy, the relationship between the input power and output power of the antenna is given as

$$P_{in} = \frac{P^2}{\rho c} A = P_{out} + Los,$$

where P_{out} is the output power and losses are to be determined (Bremstraulung, etc.).

Numerically, the estimates of the output power are computed using the acoustic power equation. The quantity P^2 is computed as

$$p_s^2 = p_{ref}^2 \bullet 10^{\frac{L_p}{10}},$$

and

$$P_{out} = \frac{P_s^2}{\rho c} A,$$

where $P_{ref}^2 = 20 \bullet 10^{-6}$, $\rho = 1.3$ kg/m^3, and $c = 333$ m/s.

Figure 14 illustrates the computer output power for acoustic levels ranging from 80 dB re 20 μPa (approximately equal to the noise from a vacuum cleaner) to 140 dB re 20 μPa (jet engine noise level).

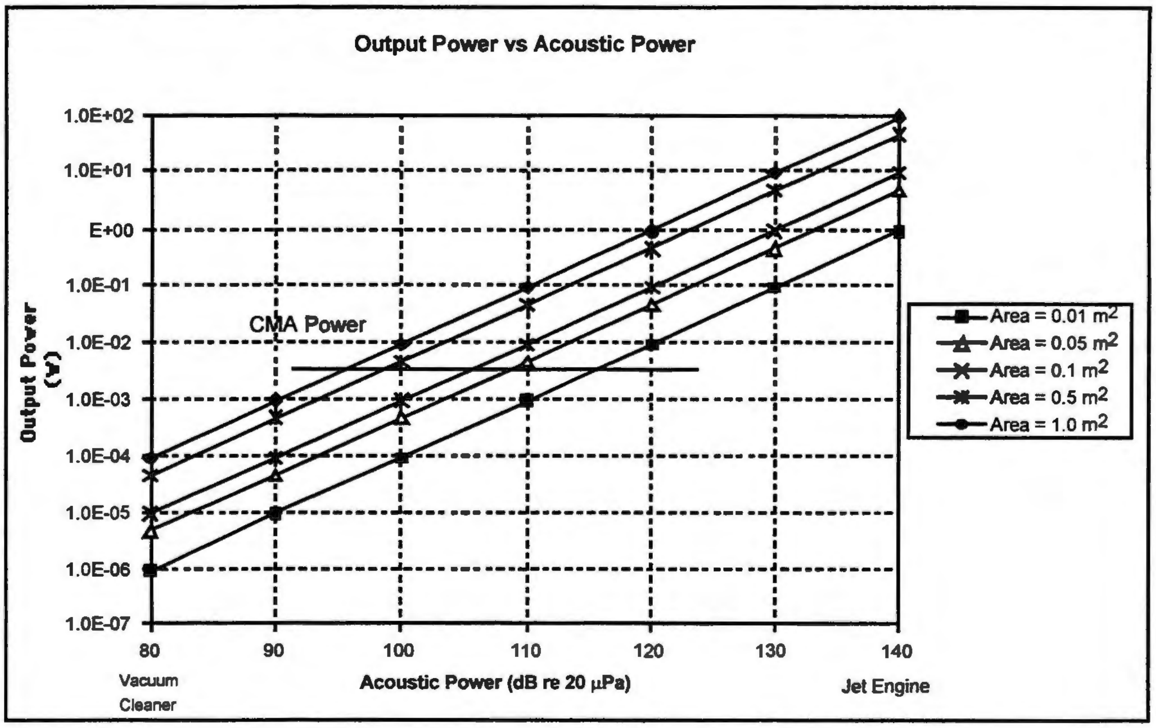

Figure 14. Output Power Density vs. Cross-Sectional Area and Input Power

Each of the curves displayed represents a different cross-sectional area. The cross sections for the computations varied from 0.01 m^2 to 1 m^{-2}. The graph shows the radiated power of the corona mode antenna (0.05 W), and the crossing point shows that the acoustic antenna will be capable of meeting radiated power requirements.

3.3 ELF PLASMA ANTENNA DRIVEN BY FOCUSED ELECTRIC FIELD

In the focused electric field design an antenna at the base of the ionized column is used to produce an oscillating electric field to drive the current carriers in the plasma at ELF. An electrostatic lens can be used to focus the antenna electric field, which otherwise would spread out too much and lose its effectiveness. A high-frequency plasma antenna, contained in a tube as an array of Hertzian dipoles, has been modeled. (The mathematical model and corresponding computer output are given in the appendix.) Each dipole is represented as an oscillating electron-ion pair—a microscopic Hertzian dipole. The effect of these atomic Hertzian dipoles is summed up over the axis of the antenna to yield a net radiative field. The Hertzian dipole design was developed for a high-frequency antenna oscillating at the resonant plasma frequency in the megahertz region and contained in a tube. The Hertzian dipole radiative mechanism can be extended to the ELF range when the oscillating ELF electric field is focused by an electrostatic lens into the ionized column. Figure 15 shows this design.

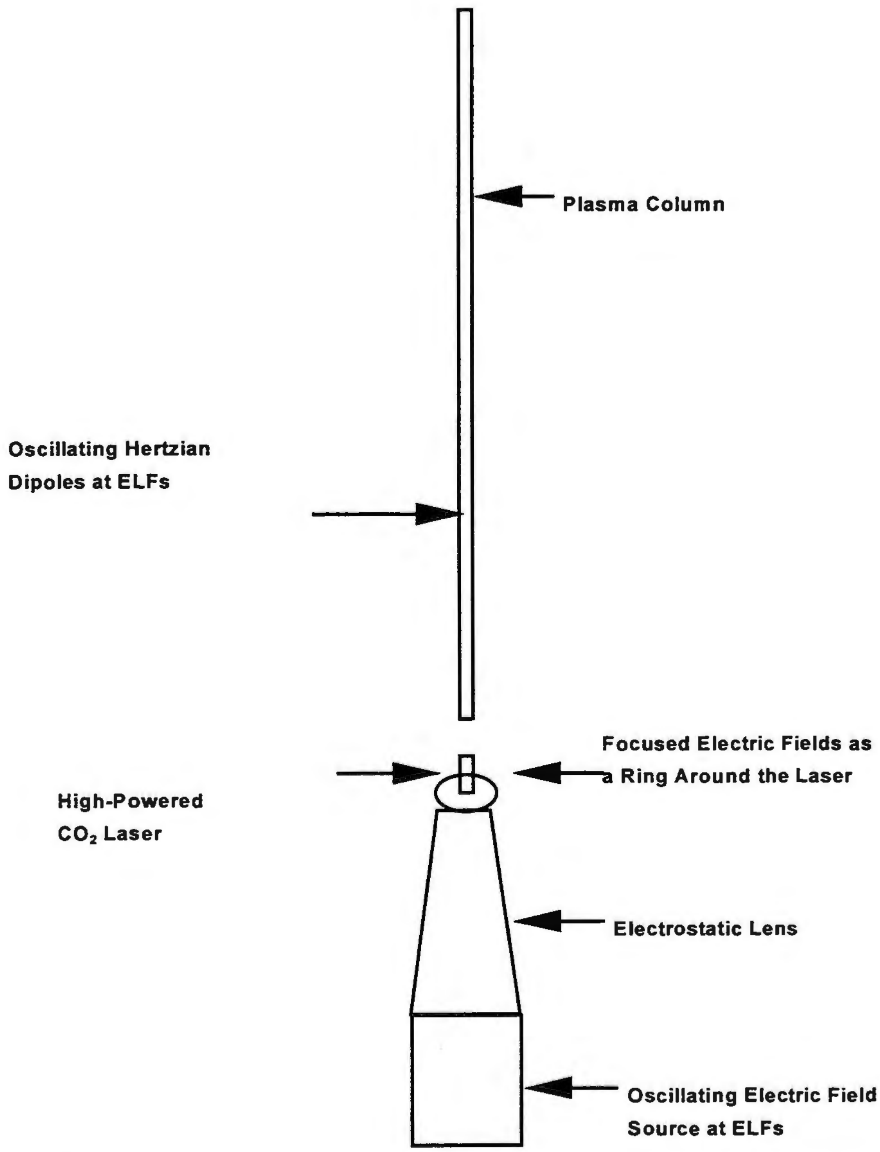

Figure 15. ELF Plasma Antenna Driven by Focused Oscillating Electric Field

4. HORIZONTAL ELF ANTENNA

The horizontal ELF antenna design is not a high priority because it is a horizontal electric dipole antenna concept (see figure 16). Because of the larger mass of ions, the current is primarily an ion current. (The mathematical model for this current appears in the appendix.) The appealing aspect of the horizontal ELF antenna design is the strong control that exists over the plasma current by an oscillating magnetic field at ELFs. This is usually called a ***drift current,*** and the direction of current motion is perpendicular to gravity and the magnetic field. As the magnetic field changes direction at ELFs, the current oscillates at ELFs with a large dipole moment, since it is primarily ion current oscillating at the plasma frequency set equal to the ELF.

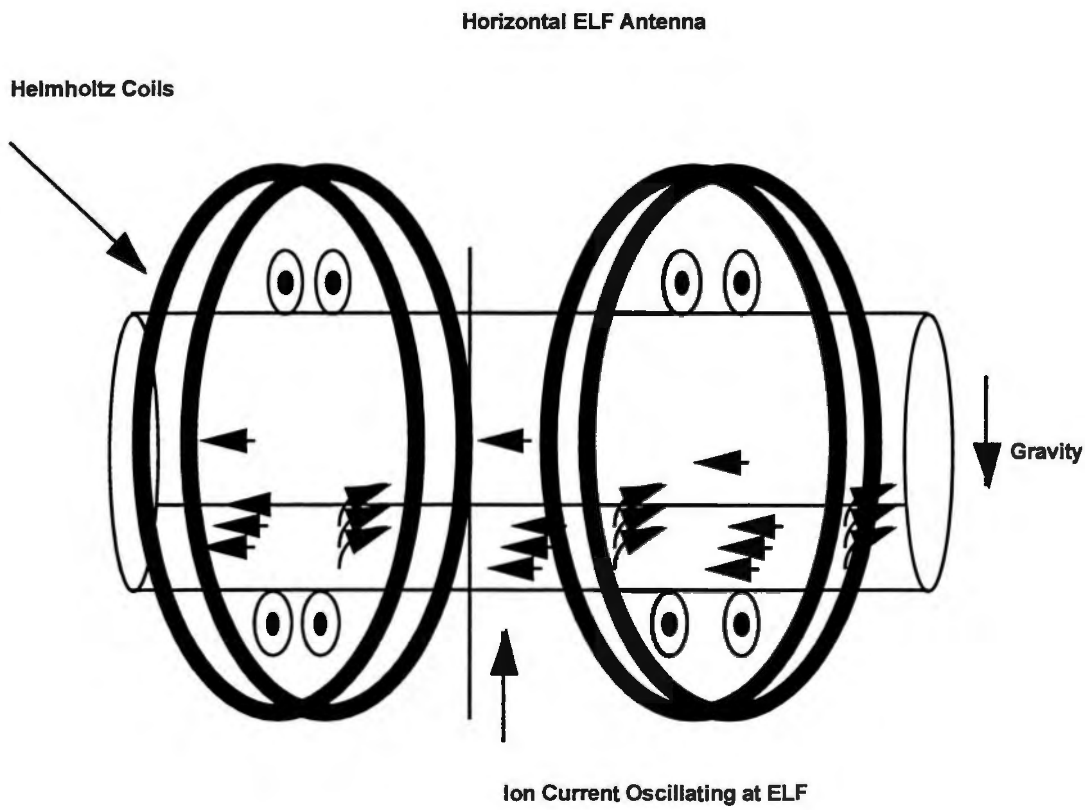

Figure 16. Horizontal ELF Antenna

The drift velocity of charged particles due to gravity is given as

$$\vec{v}^{\alpha}_{DG} = \frac{m_\alpha}{q_\alpha}\frac{\bar{g}\times\bar{B}}{B^2}c,$$

where $a = e$ for electrons and $a = i$ for ions. From examination of this equation, the following conclusions can be drawn:

- Ions and electrons drift in opposite directions.
- Ions have a velocity that is $\frac{m_i}{m_e}$ > velocity of electrons.
- Ions drift from electrons, causing a charge separation and an electric field.

Let $\overset{r}{B}$ oscillate at frequency $w = 100$ kHz, then

$$\vec{B} = \text{Re}\,\hat{\vec{B}}e^{j\omega t},$$

$$v_{DG}^{\alpha} = \frac{m_\alpha}{q_\alpha}\frac{\vec{g}\times \text{Re}\,\hat{\vec{B}}e^{j\omega t}}{B^2}c,$$

$$v_{DG}^{\alpha} = \text{Re}\left[\frac{m_\alpha}{q_\alpha}\frac{\vec{g}\times \text{Re}\,\hat{\vec{B}}}{B^2}\right]e^{j\omega t}.$$

Therefore, the drift velocity oscillates at the magnetic field frequency, and the electrons and ions oscillate in opposite directions, providing current.

5. CONCLUSIONS

All the designs proposed in this report have the potential for transmitting and receiving radiation patterns—even though the physical mechanisms for each case are, to varying degrees, different. The ELF plasma antenna models and the high-frequency Hertzian dipole model are intertwined. The high-frequency plasma antenna model and the more difficult ELF model should be developed concurrently; insights gained from the high-frequency model work will be useful in development of the ELF model.

The plasma ELF antenna has a tremendous advantage over the horizontal electric dipole ELF antenna, which lacks portability and efficiency. The vertical electric dipole ELF antenna is supported by a balloon at least 12,000 feet high, is extremely cumbersome, and lacks portability. Furthermore, a balloon-supported metallic antenna is not stealthy. The ELF plasma antenna is portable, more efficient (because of its extensive use of focused laser light), and stealthy.

This report is intended to stimulate research and development of the ELF plasma antenna.

APPENDIX

SUPPORTING CALCULATIONS

FARFIELD RADIATION OF AN OSCILLATING PLASMA: ROUSSEL-DUPRÉ MODEL

The nonlinear interactions occur to the dynamics of the plasma itself. An analysis by Roussel-Dupré and Miller has shown that the normalized radiated electric field for a plasma cloud (or column) is given as

$$\widetilde{E}(s,x,z) = e^{-x^2/D^2}\left(\int_{-\infty}^{z} dz' \frac{s}{c^2}\left[e_0\alpha_0(s,z')e^{i\int_{z'}^{z} k_{z''}^{0} dz''} + e_1\alpha_1(s,z')e^{i\int_{z'}^{z} k_{z''}^{1} dz''}\right]\right)$$

$$+ e^{-x^2/D^2}\left(\int_{-\infty}^{z} dz' \frac{s}{c^2}\left[e_0\alpha_0(s,z')e^{-iz''\int^{z} k_{z''}^{0} dz''} + e_1\alpha_1(s,z')e^{-i\int_{z'}^{z} k_{z''}^{1} dz''}\right]\right),$$

where

$$\alpha_0 = \frac{s_2\beta_2^{\;2} + \beta\left(\dfrac{c^2}{D^2} + \sqrt{\dfrac{c^4}{D^4} - s^4\beta_2^2}\right)}{4ik_{z'}^{0}\sqrt{\dfrac{c^4}{D^4} - s^4\beta_2^2}},$$

$$\alpha_1 = \frac{s_2\beta_2^{\;2} + \beta\left(\dfrac{c^2}{D^2} + \sqrt{\dfrac{c^4}{D^4} - s^4\beta_2^2}\right)}{4ik_{z'}^{0}\sqrt{\dfrac{c^4}{D^4} - s^4\beta_2^2}},$$

$$k_x^0 = \left[\left(\frac{1}{D^2} + i\frac{s^2}{c^2}\beta_2\right) - \sqrt{\frac{1}{D^4} - \frac{s^4}{c^4}\beta_2^2}\right]^{1/2},$$

$$k_x^1 = \left[\left(\frac{1}{D^2} + i\frac{s^2}{c^2}\beta_2\right) - \sqrt{\frac{1}{D^4} - \frac{s^4}{c^4}\beta_2^2}\,\right]^{1/2},$$

$$e^0 = \begin{bmatrix} 1 \\ \dfrac{s^2\beta_2}{\dfrac{c^2}{D^2} + \sqrt{\dfrac{c^2}{D^4} - s^4\beta_2^2}} \\ 0 \end{bmatrix},$$

$$e^1 = \begin{bmatrix} 1 \\ \dfrac{s^2\beta_2}{\dfrac{c^2}{D^2} + \sqrt{\dfrac{c^2}{D^4} - s^4\beta_2^2}} \\ 0 \end{bmatrix},$$

$$\beta = \frac{4\pi\sigma_p e^{-z^2/d^2}}{s},$$

$$\beta_2 = \frac{4\pi\sigma_H e^{-z^2/d^2}}{s},$$

where D is the length of plasma, and s is the frequency.

The magnitude of the field is normalized to V_0B_0/c, where V_0 is the initial plasma velocity, B_0 is the background magnetic field strength, and c is the speed of light. Therefore, the magnitude of the radiated wave is directly influenced by the magnetic field and the plasma velocity.

Roussel-Dupré's work has also shown that the radiated EM wave will have the same frequency as the plasma wave. Further, in their work the plasma cloud or column behaved as a dipole, producing the pattern illustrated in figure A-1.

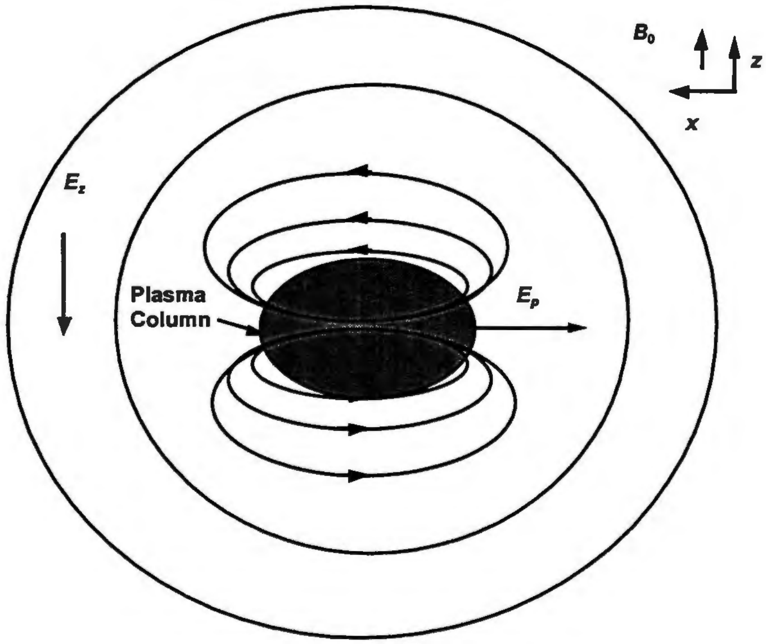

Figure A-1. Radiation Pattern of Plasma Column

Numerical analyses performed by Roussel-Dupré and Miller have produced the values for the normalized field. Measurements and calculations on EM emissions from plasmas have varied significantly. Roussel-Dupré's work has suggested that emissions were on the order of 25 mV/m at 1.6 km. At the other extreme, measurements on electrostatic discharges (1/2-in. arc, 26 A) have produced radiated electric fields on the order of 150 V/m at 1.5 m.

RADIATED FIELD FROM PLASMA OSCILLATIONS: MHD MODEL

Others have shown mathematically that plasma oscillations are also responsible for radiating EM fields. Montgomery and Tidman (1964) have shown that the basic cold plasma equations are

$$\frac{\partial n}{\partial t}+\frac{\partial}{\partial x}\bullet(nv)=0 \qquad \frac{\partial v}{\partial t}+v=-\frac{e}{m}\left(E+\frac{1}{c}v\times B\right),$$

$$\frac{\partial}{\partial x}\times E=-\frac{1}{c}\frac{\partial B}{\partial t} \qquad \frac{\partial}{\partial x}\bullet E=4\pi e(N_0-n),$$

$$\frac{\partial}{\partial x}\times B=\frac{1}{c}\frac{\partial E}{\partial t}-\frac{4\pi e}{c}nv \qquad \frac{\partial}{\partial x}\bullet B=0,$$

where N_0 is the ion density, $n(x,t)$ is the density of zero temperature electron gas, and $v(x,t)$ is the velocity. Montgomery and Tidman (1964) use a perturbation scheme to develop a set of coupled equations. The equations are solved to determine the radiated field, and the solution is divided into first- and second-order solutions. The first-order electric field is (Ginsburg, 1964):

$$E = \frac{\partial \phi}{\partial x} \sin(\omega_e t) + A_T \sin(vt - K \bullet x + \alpha).$$

The second term of this equation represents the transverse component of the electric field. The velocity of the wave is given as

$$v_2 = K_2 c_2 + \omega_e^2,$$

where $K \bullet A_t = 0$. The corresponding magnetic field is given as

$$B = \frac{c}{v} K \times A_T \sin(vt - K \bullet x + \alpha).$$

The source size of the plasma oscillation must also be defined and is given as

$$\phi = \phi_0 (1 + \delta \bullet x) e^{-x^2/L^2},$$

where *d* is the deviation from spherical symmetry, and *L* is the thickness of the plasma slab.

The magnetic field at a distance *x* from the plasma is then given as (Ginsburg,1964)

$$B = \frac{e\kappa^2 \phi_0^2 \sqrt{\pi} L^3}{32\sqrt{2} mc\omega_e} (\delta \bullet n)(\delta \times n) \frac{\sin(2\omega_e t - \kappa x)}{x} e^{-3\omega_e^2 L^2/8c^2},$$

where **n** is the gas density function of *x* position and time, **e** is the electron charge, **m** is the electron mass, N_0 is the ion density, ϕ is the source size, ω_e is the electron frequency, ω_e is

$\sqrt{\left(\frac{4\pi N_0 e^2}{m}\right)}$, and κ is the wave number $= \frac{\sqrt{3}\omega_e}{c}$.

Since the electric field is related to the magnetic field via $E = \eta H$, it is obvious that the radiated electric field is also a function of the plasma electron frequency. The frequency of the second-order magnetic field is equal to twice the plasma frequency and is valid when $\omega_e L \leq c$.

Similar equations can be obtained using the plasma ion frequency instead of the electron frequency. The ion frequency is believed to have a more pronounced effect because the ion mass is significantly greater than an electron mass.

ELF PLASMA ANTENNA PRELIMINARY CURRENT PREDICTIONS

A 1-kW carbon dioxide laser with a beamwidth of 2 mm produces 3.18 billion w/m^2 of energy intensity. If this converts to pure radiation intensity in the farfield, then the energy intensity in the laser is equal to the farfield Poynting vector. The farfield Poynting vector is equal to the square of the *H* field times the characteristic impedance. The characteristic impedance is numerically 377. Setting the square of the *H* field times the characteristic impedance equal to the laser intensity, we can solve for the *H* field and get 56,000 A/m. Using Amperes law and choosing somewhat arbitrarily the ELF distance as 4000 m as the length of the antenna, we set the product of the *H* field and the antenna length equal to the current carried by the plasma antenna. We obtain several hundred amps, which is a far greater current than can be carried by a metal antenna. Of course, this result depends on 100-percent conversion of the laser energy into the farfield ELF plasma radiation; however, if the energy conversion is only a few percent, this is much more current than can be generated on a metallic antenna.

RELAXATION TIMES

When the atmosphere is ionized with lasers, the electrons and ions relax to separate Maxwellian distributions because of the difference in kinetic energy and gravitational potential energy. The Maxwellian distributions for electrons and ions (Roussel-Dupré, 1993b) are given as:

Electrons:

$$f_e = \left(\frac{m_e}{2\pi kT}\right)^{3/2} e^{-(m_e v^2 + m_e gh)/2kT} .$$

Ions:

$$f_i = \left(\frac{m_i}{2\pi kT}\right)^{3/2} e^{-(m_i v^2 + m_i gh)/2kT} .$$

The relaxation times for electrons and ions (Roussel-Dupré and Miller, 1993b) are given as:

Electrons:

$$\tau_e \approx \frac{m_e e^{1/2} (2kT_e)^{3/2}}{8\pi n_e e^4 \left[\Phi(1) - 4e^{-1}/\sqrt{\pi}\right] \ln \Lambda},$$

Ions:

$$\tau_i \approx \frac{m_i e^{1/2}(2kT_i)^{3/2}}{8\pi n_i e^4\left[\Phi(1) - 4e^{-1}/\sqrt{\pi}\right]\ln\Lambda},$$

where

$$\Phi(y) = \frac{2}{\sqrt{\pi}}\int_0^y e^{-x^2}dx,$$

and

$$\Lambda = \frac{3}{2}\left(\frac{k^3T^3}{\pi n}\right)^{1/2}\frac{1}{ze^2}.$$

The net current density from relaxation time is

$$J = \frac{n_i}{\tau_i} + \frac{n_e}{\tau_e}.$$

From Krall and Trivelpiece (1973, p. 306), the relaxation times for gas discharges, with densities on the order of 10^{14} cm^{-3} (similar to those computed for our ionized plasma column), are on the order of 2×10^{-9}s for electrons and 2×10^{-7}s for ions. This suggests that the transient current generated is on the order of

$$J = \frac{10^{14}}{2 \bullet 10^{-9}} + \frac{10^{14}}{2 \bullet 10^{-7}}.$$

The result is obtained by multiplying the above equation by 1.6×10^{-19} coulombs. The current per-unit volume is then 8,080 A/cm^3. The current density is then computed by multiplying the volume by a length. Assuming a 1-cm length (i.e., the length between spheres), the current density is 8,080 A/cm^2. The results of this analysis suggest that each ionized sphere must be revisited on the order of 10^{-9} s.

The pulse durations for some common lasers, in the mode locked operation, are as follows:

Laser Type	**Pulse Duration (s)**
He-Ne	6×10^{-10}
Nd:YAG	7.6×10^{-11}
Ruby	1.2×10^{-11}

When ionization occurs, $t_e = 10^{-8}$ s is the relaxation time for electrons to the Maxwell-Boltzman statistics of electrons. During this time t_e, the electrons move in the z direction with respect to the air molecules, coming from

$$\langle z \rangle_e - \langle z \rangle_{air},$$

where

$$\langle z \rangle_e = \frac{\int_0^z z\rho_e e^{-m_e z/kT_e}}{\int_0^z \rho_e e^{-m_e z/kT_e}},$$

and

$$\langle z \rangle_{air} = \frac{\int_0^z z\rho_{air} e^{-m_{air} z/kT_{air}}}{\int_0^z \rho_{air} e^{-m_{air} z/kT_{air}}},$$

where r_e is the density of electrons at sea level, and r_{air} is the density of air at sea level. The relaxation time for ions is t_e @ 10^{-7}s and will not be included in this approximation.

$m_e = 9.11 \times 10^{-31}$ kg, mass of an electron,
$T = 300$ K,
T_e = electron temperature (to be determined), and
m_{air} = the weighted mass of an air molecule.

Hence the electron current that exists over time t_e @ 10^{-9} s is

$$\frac{n_e \left| \langle z \rangle_e - \langle z \rangle_{air} \right|}{\tau_e}.$$

If a pulsed laser can be synchronized with the recombination time t_e such that

$$\tau_{pulse} = \frac{2l}{cN} \approx \tau_e + \tau_c,$$

the mode number N and laser length l to give "continuous" current can be determined.

ZERO RADAR CROSS SECTION OF ELF PLASMA ANTENNA COLUMN

One of the added benefits of the plasma antenna is a reduced radar cross section. This is important to submarines if the antenna is mounted on top of the mast or combined as a conformal antenna on a stealth sail, but it is probably of greater importance to the surface ship community, where the antennas tend to be relatively large and can contribute significantly to the size of the ship cross section.

This section describes the methods by which EM waves are transmitted and reflected by the plasma antenna. The generic antenna configuration is illustrated in figure A-2.

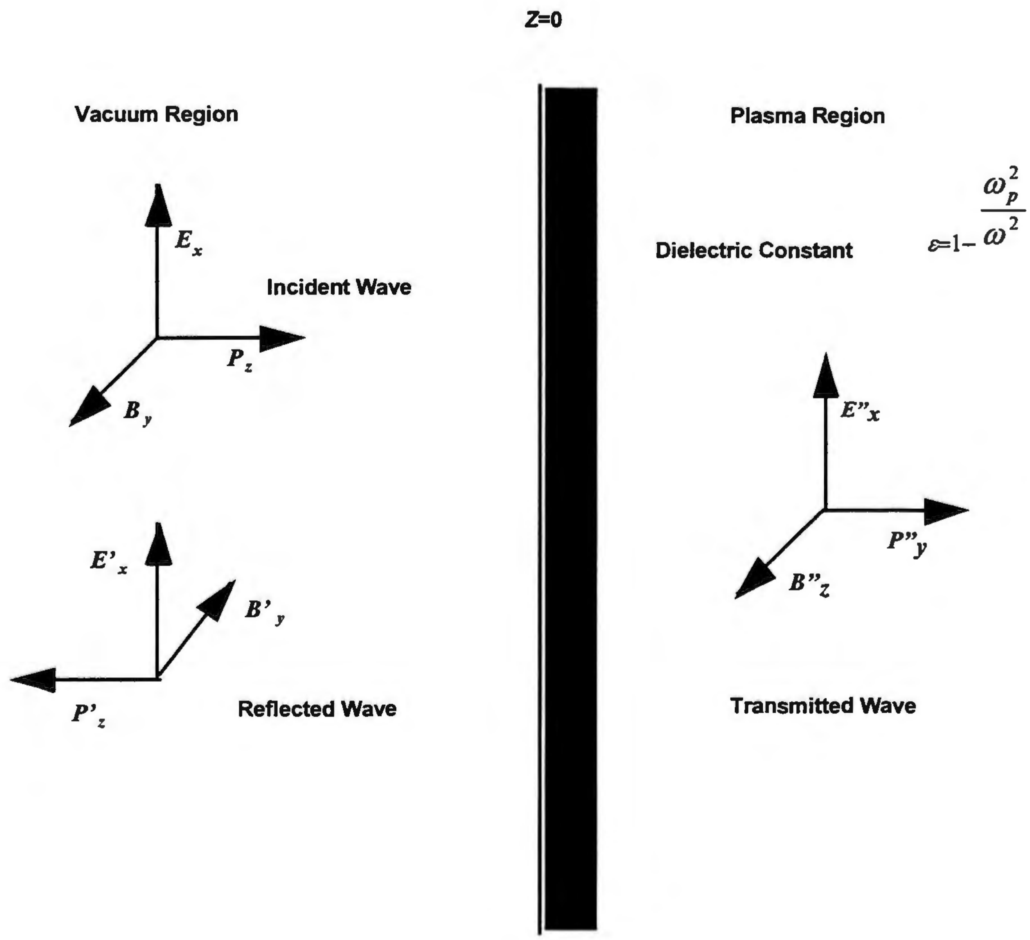

Figure A-2. Wave Reflection at Vacuum/Plasma Interface

The boundary between the vacuum and the plasma region is depicted at $Z = 0$. The electric and magnetic field components of the incident wave are given as

$$E_x = E_{x0} e^{+ik_0 z} \qquad B_y = E_{x0} e^{+ik_0 z},$$

where E_{xo} is the amplitude of the incident wave. The components of the reflected wave are given as

$$E'_x = RE_{x0} e^{+ik_0 z} \qquad B_y = RE_{x0} e^{+ik_0 z},$$

where R is the reflection coefficient. The transmitted wave components are

$$E''_x = TE_{xo} e^{+ik_0 z} \qquad B''_y = T \frac{E_{xo} k_p c}{\omega} e^{+ik_0 z},$$

where T is the transmission coefficient.

The relationships between the wave numbers, frequencies in a vacuum and in the plasma, are given as

$$k_0^2 c^2 = \omega^2 \text{ (vacuum)},$$

$$k_p^2 c^2 = \omega^2 \left(1 - \frac{\omega_p^2}{\omega^2}\right) \text{ (plasma)},$$

where k_p is the wave number in plasma, k_0 is the wave number in a vacuum, w_p is the plasma frequency, and w_0 is the frequency in vacuum.

The reflection coefficient is given as

$$R = \frac{k_0 - k_p}{k_0 + k_p},$$

and the transmission coefficient as

$$T = \frac{2k_0}{k_0 + k_p}.$$

Using the relationships between the plasmas and the vacuum, the conditions listed in table A-1 are evident. Table A-1 shows that for high-frequency waves, there will be perfect transmission. Thus, as long as the plasma antenna is operating at frequencies below that of search radar, the radar cross section of the plasma antenna will be less than an equivalent metallic antenna. As an example, consider the case where the plasma antenna is transmitting at a frequency of 30 MHz and is scanned by a radar operating at 3 GHz. The amount of reflected energy would be on the order of 0.047 percent.

Table A-1. Reflection and Transmission Coefficients vs. Frequency

Frequency	R	T	Comment
High ($w >> w_p$)	0	1	Perfect transmission
$w^3 w_p$	$0<R<1$	$0<T<2$	Partial transmission, partial reflection
$w = w_p$	1	2	Oscillations
Low ($w << w_p$)	-1	0	Perfect reflection

HERTZIAN DIPOLE ARRAY MODEL OF PLASMA ANTENNA WITH COMPUTER OUTPUT

The radiated electric field produced by a line of charges in the plasma is calculated by modeling electron/ion pairs as Hertzian dipoles. The total radiated field is then the summation of the fields radiated by each individual dipole.

The force on an electron in a time-varying, harmonic electric field $\left(\vec{E}\right)$ is given as

$$\vec{F} = -e\vec{E},$$

where $e = 1.6\times10^{-19}\,C$. The force is also expressed as

$$\vec{F} = m\frac{d^2x^2}{dt^2} = m\omega^2\vec{x},$$

where m is mass, and ω is the angular frequency.

The dipole moment, N_{dip}, is equal to the charge times the distance between the charged particles, as illustrated in figure A-3.

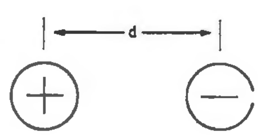

Figure A-3. Distance Between Charged Particles

Mathematically, the dipole moment is given as $N_{dip} = qd$. The dipole moment per unit volume p is given as

$$\vec{p} = -Ne\vec{x},$$

where N is the number of electrons in the plasma per unit volume:

$$\vec{p} = -\frac{Ne^2}{m\omega^2}\vec{E}.$$

D is given as

$$\vec{D} = \varepsilon_0 \vec{E} + \vec{p} = \varepsilon_0 \vec{E} - \frac{Ne^2}{m\omega^2}\vec{E}.$$

Simplifying the equation yields

$$\vec{D} = \varepsilon_0 \left[1 - \frac{\omega_p^2}{\omega^2}\right]\vec{E},$$

where $\omega_p = \sqrt{\frac{Ne^2}{m\varepsilon_0}}$ is the plasma frequency.

In this application, the Hertzian dipoles are formed by two charged particles, as illustrated on the left-hand side of figure A-4. At a time $t = T/4$, the current flows between the charges until the charge on the particles is reversed ($t = T/2$). The current then changes direction as the charges again reverse themselves between the two particles.

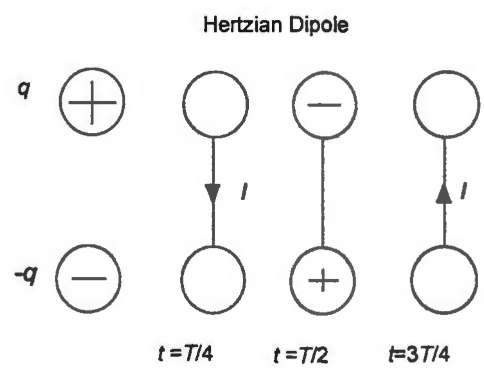

Figure A-4. Hertzian Dipole

The insertion loss (IL) product for these miniature dipoles is given as

$$|\Delta z = j\omega p,$$

where $p = qDz$. The electric and magnetic field components for a Hertzian dipole are given as

$$\overset{v}{E} = 0\sqrt{\frac{N}{\varepsilon}}\, j\frac{kI\Delta z e^{-jkr}}{4\pi}\sin\theta ,$$

and

$$\overset{r}{H} = \phi j\frac{kI\Delta z e^{-jkr}}{4\pi r}\sin\theta .$$

The electric and magnetic fields are perpendicular to each other. The wave impedance is given as

$$\eta = \sqrt{\frac{\mu}{\varepsilon}} .$$

The length between the charged particles is computed by

$$900\ \text{MHz} = \frac{\omega_p}{2\pi} = \sqrt{\frac{n(1.6 \bullet 10^{-19})^2}{9.11 \bullet 10^{-31})(8.85 \bullet 10^{-12})}} ,$$

where $n = 10^{18}$ electrons/m^3. The linear spacing of the electrons is then given as spacing $= \sqrt[3]{n}$. Substituting values yields an approximate spacing of 1 mm. Thus, Dz = 1 mm.

If the antenna is 1 cm long, and operating at 900 MHz, then the sum of the Dz from -0.5 cm to 0.5 cm should yield the desired pattern for the single line of ion/electron pairs. Based on the coordinate system found in figure A-5, the field is given as

$$\left|\overset{r}{E}\right| = \sqrt{\frac{\mu}{\varepsilon}}\frac{|I|\Delta z}{4\pi r}|\sin\theta| ,$$

and the Poynting vector is then given as

$$\langle s\rangle = \frac{1}{2}\mathrm{Re}\left[\vec{E}\times\vec{H} = \vec{r}\,\frac{1}{2}\sqrt{\frac{\mu}{\varepsilon}}\left|H_\theta\right|^2 = \vec{r}\,\frac{\eta}{2}\left(\frac{k|I|\Delta z}{4\pi r}\right)^2 \sin^2\theta\ .\right.$$

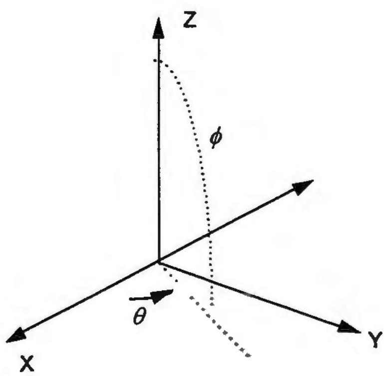

Figure A-5. Coordinate System for Plasma Model

BIBLIOGRAPHY

Allis, W., *Wave in Anisotropic Plasmas*, MIT Press, Cambridge, MA, 1963.

Auld, B., "Signal Processing in a Nonperiodically Time-Varying Magnetoelastic Medium," *Proceedings of the IEEE*, vol. 6, no. 3, 1968.

Bolz, R., *CRC Handbook of Tables for Applied Engineering Science*, CRC Press, 1976.

Booker, H. G., *Cold Plasma Waves*, Kluwer Press, Hingham, MA, 1984.

Case, K., "Radiation from a Slot Antenna in a Ground Plane Coated with a Moving Plasma Sheath," *IEEE Transactions on Antennas and Propagation*, vol. 19, no. 3, 1971.

Felson, L., and G. Whitman, "Wave Propagation in Time Varying Media," *IEEE Transactions on Antennas and Propagation*, vol. 18, no. 2, 1970.

Fischer, B., "Helicon Wave Coupling to a Finite Plasma Column," Institut fur Experimentalphysik II, Ruhr-Universitat Bochum, March 1994.

Ginsburg, A., *The Propagation of Electromagnetic Waves in Plasmas*, John Wiley and Sons, New York, 1964.

Glanz, J., "Electromagnetic Instability and Emissions from Counterpropagating Langmuir Waves," *The Physics of Fluids B*, vol. 5, no. 4, 1993.

Halliday, D., and R. Resnick, *Fundamentals of Physics*, John Wiley and Sons, New York, 1986.

Hatt, W., "Radiation from an Aperture in a Conducting Plane Coated with a Moving Plasma Layer," Masters Thesis, Air Force Institute of Technology, Wright Patterson Air Force Base, OH, March 1970.

Jarem, J., "The Input Impedance of Antenna Characteristics of a Cavity-Backed Plasma Covered Ground Plane Antenna," *IEEE Transactions on Antennas and Propagation*, vol. 34, no. 2, 1986.

Kalluri, D., "Effects of Switching a Magnetoplasma Medium on a Traveling Wave: Longitudinal Propagation," *IEEE Transactions on Antennas and Propagation*, vol. 37, no. 12, 1989.

Kashiwa, T., "Transient Analysis of Magnetized Plasma in Three-Dimensional Space," *IEEE Transactions on Antennas and Propagation*, vol. 36, no. 8, 1988.

Kojima, T., and T. Higashi, "Electromagnetic Radiation from a Slot Antenna Surrounded by a Moving Magnetoplasma Sheath," *Radio Science*, vol. 8, no. 12, 1973.

Krall, N., and A. Trivelpiece, *Principles of Plasma Physics*, McGraw-Hill, New York, 1973.

Lewis, J., "Asymptotic Theory of Electromagnetic Wave Propagation in Inhomogeneous Anisotropic Plasma," Report 090187, New York University, October 1969.

Lui, C., "Electromagnetic Oscillating Two-Stream Instability of Plasma Waves," Report MD-TR-80-103, University of Maryland, May 1980.

Meger, R., "Experimental Investigations of the Formation of Plasma Mirror for High-Frequency Microwave Beam Steering," *Physics of Plasmas*, vol. 2, no. 6, 1995.

Montgomery, D., and D. Tidman, *Plasma Kinetic Theory*, McGraw-Hill, New York, 1964.

Nordwall, B., "Navy Research Laboratory Tests Plasma Antenna," *Aviation Week and Space Technology*, June 10, 1996.

Pierce, A., *Acoustics: An Introduction to Its Physical Principles and Application*, American Institute of Physics, 1989.

"Plasma Antenna in a Nuclear Environment," American Nucleonics Corporation Report DSA-1733 (prepared for the Defense Atomic Support Agency), 7 October 1965.

Roussel-Dupré, R., and R. Miller, "Radiative Properties of a Plasma Moving Across a Magnetic Field 1, Numerical Results," *The Physics of Fluids*, B, vol. 5, no. 4, 1993a.

Roussel-Dupré, R., and R. Miller, "Radiative Properties of a Plasma Moving Across a Magnetic Field 1, Theoretical Results," *The Physics of Fluids B*, vol. 5, no. 4, 1993b.

Tidman, D., and G. Weiss, "Radio Emission by Plasma Oscillations in Nonuniform Plasmas," *The Physics of Fluids*, vol. 4, no. 6, 1961.

Tidman, D., and G. Weiss, "Radiation by a Large-Amplitude Plasma Oscillation," *The Physics of Fluids*, vol. 5, no. 7, 1962.

Van Valkenburg, M., *Reference Data for Engineers, Radio, Electronics, Computer, and Communications*, 8th Edition, SAMS Publishing, New York, 1993.

Ward, M., "Tubular Antenna in a Plasma Transform Technique," Report HVD-TR-632, Harvard University, 1972.

Ward, M., "Cylindrical Antenna in a Hot Plasma: A General Analysis Including Longitudinal Wave Excitation Effects," Report HVD-TR-648, Harvard University, 1973.

Weil, C., "Radiation Characteristics of Planar Rectangular Apertures Covered by a Layer of Moving Cold Plasma," *IEEE Transactions on Antennas and Propagation*, vol. 37, no. 9, 1989.

DISTRIBUTION LIST

Internal Codes:	10 (R. Nadolink) 102 (S. Dickinson) 2141 (W. Keith) 34 (P.M. Trask) 34A (J.F. Boucher) 341 (G.M. Exley) 3412 (R.C. Olesen) 3413 (J. Casey) 3414 (S.C. Stefanowicz) 3421 (W.P. Huntley) 3422 (H. Anderson, G.E. Holmberg) 343 (D.S. Dixon) 3431 (T. Anderson (20), C.F. Derewiany) 3432 (B.C. Eccles) 3433 (T.R. Floyd) 3491 (R.J. Aiksnoras) 3492 (P.S. Sheldick) 3493 (C.E. McMillan) 3495 (J. Perry) 3496 (F.C. Allard) 3497 (C.M. Floyd) 3498 (C. Amidon) 5441 (2)
Total:	46